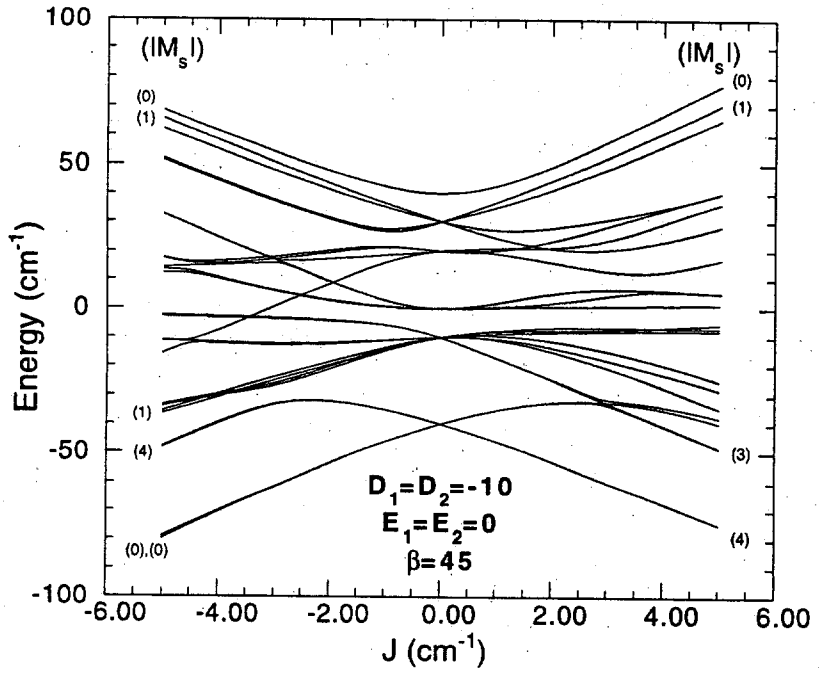

Figure S1. Correlation diagram of the energy levels of the binuclear ferrous ground state including exchange coupling, single-site ZFS and noncollinearity between the two iron atoms. The axial ZFS parameters (D) of the two iron atoms are held negative, constant and equal ($D_1 = D_2 = -10$ cm^{-1}). The exchange coupling (J) is varied from -5 to +5 cm^{-1}. One iron rotates 45° from the other ($\beta = 45°$). The right side indicates a ferromagnetic interaction ($J > 0$) between the ferrous atoms, and the left an antiferromagnetic interaction ($J < 0$). The spin Hamiltonian used for calculating the levels is given in Eq. 1, with $H_x = H_y = H_z = 0$.

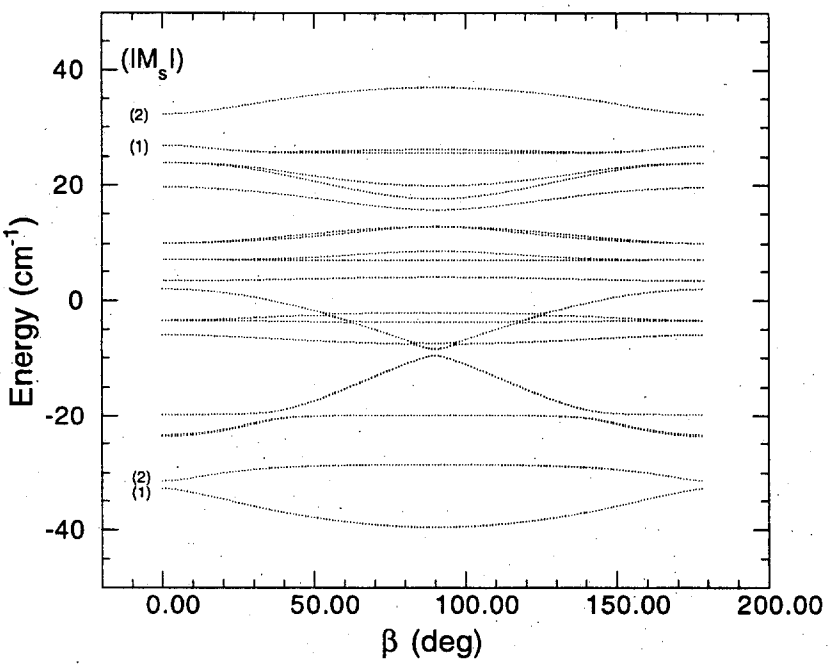

Figure S2. Correlation diagram of the energy levels of the binuclear ferrous ground state including exchange coupling, single-site ZFS and noncollinearity between the two iron atoms. The axial ZFS parameters (D) of the two iron atoms and the exchange coupling (J) are held constant ($D_1 = -10$ cm^{-1}, $D_2 = +5$ cm^{-1} and $J = -1.5$ cm^{-1}). The angle between the two irons varies from 0 to 180 degrees. The spin Hamiltonian used for calculating the levels is given in Eq. 1, with $H_x = H_y = H_z = 0$.

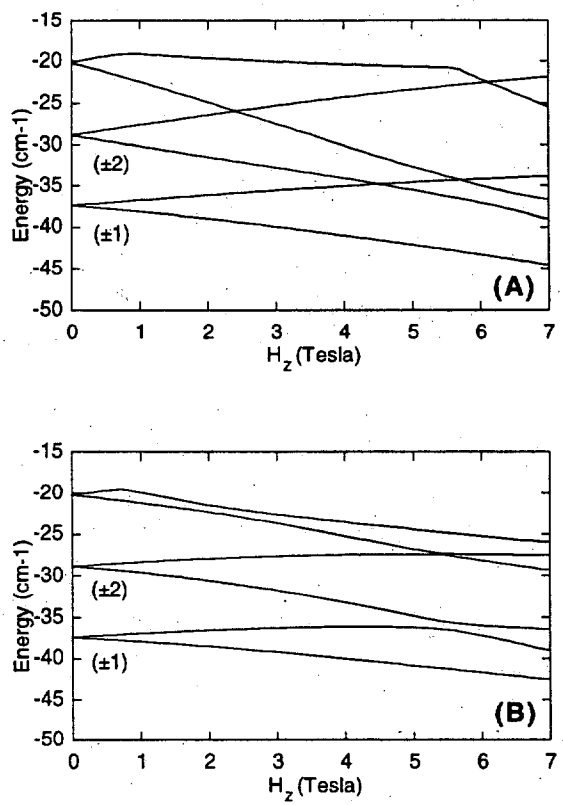

Figure S3. Representative correlation diagrams of the energy splittings of the binuclear ferrous ground and excited sublevels with positive ZFS in the presence of a magnetic field along the z-axis. The axial and rhombic ZFS parameters on the two iron atoms and the exchange coupling are held constant as $D_1 = -10\ cm^{-1}$, $D_2 = +5\ cm^{-1}$, $J = -1.5\ cm^{-1}$. The angle between the two irons (β) is fixed at: (A) $\beta = 45°$ and (B) $\beta = 135°$. The spin Hamiltonian used for calculating the levels is given in Eq. 1, with $H_x = H_y = 0$ and H_z varied from 0 to 7 Tesla.

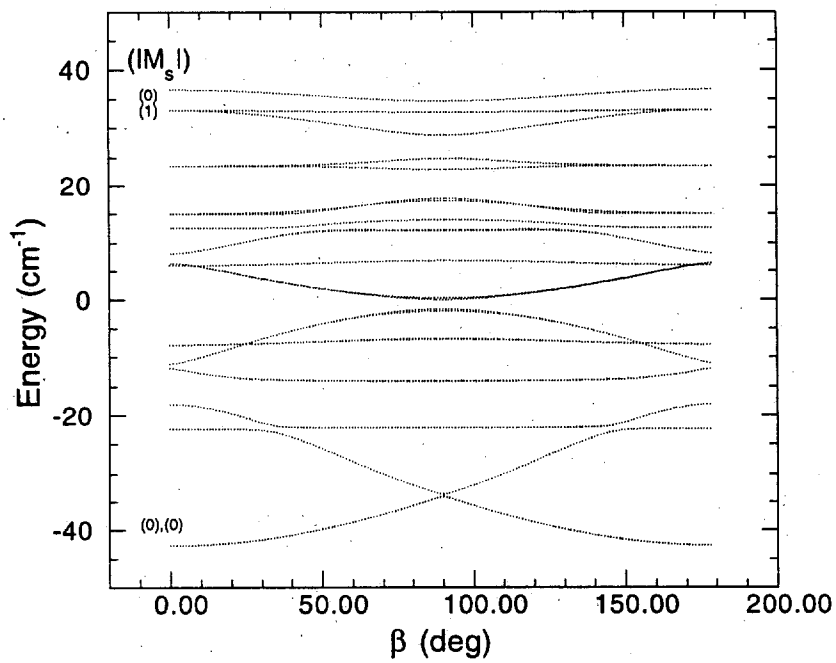

Figure S4. Correlation diagram of the energy levels of the binuclear ferrous ground state including exchange coupling, single-site ZFS and noncollinearity between the two iron atoms. The axial ZFS parameters (D) of the two iron atoms and the exchange coupling (J) are held constant ($D_1 = -10$ cm^{-1}, $D_2 = -5$ cm^{-1} and $J = -1.5$ cm^{-1}). The angle between the two irons varies from 0 to 180 degrees. The spin Hamiltonian used for calculating the levels is given in Eq. 1, with $H_x = H_y = H_z = 0$.

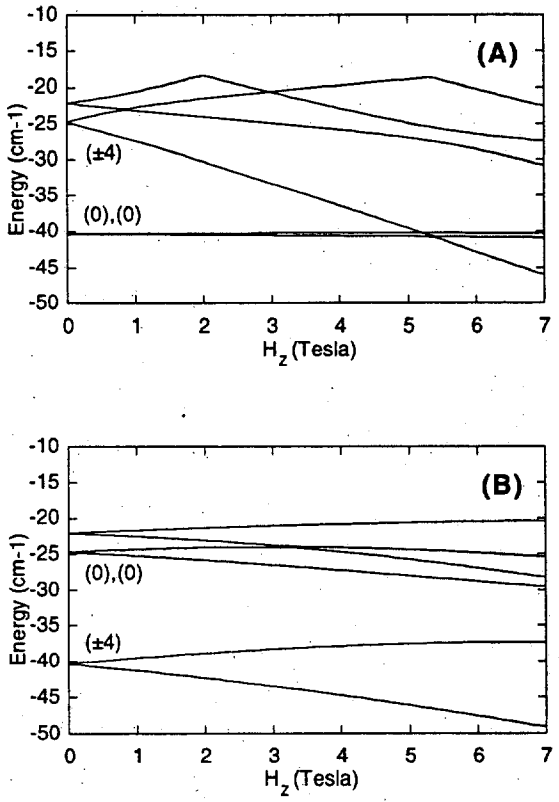

Figure S5. Representative correlation diagrams of the energy splittings of the binuclear ferrous ground and excited sublevels with positive ZFS in the presence of a magnetic field along the z-axis. The axial and rhombic ZFS parameters on the two iron atoms and the exchange coupling are held constant as $D_1 = -10\ cm^{-1}$, $D_2 = -5\ cm^{-1}$, $J = -1.5\ cm^{-1}$. The angle between the two irons (β) is fixed at: (A) $\beta = 45°$ and (B) $\beta = 135°$. The spin Hamiltonian used for calculating the levels is given in Eq. 1, with $H_x = H_y = 0$ and H_z varied from 0 to 7 Tesla.

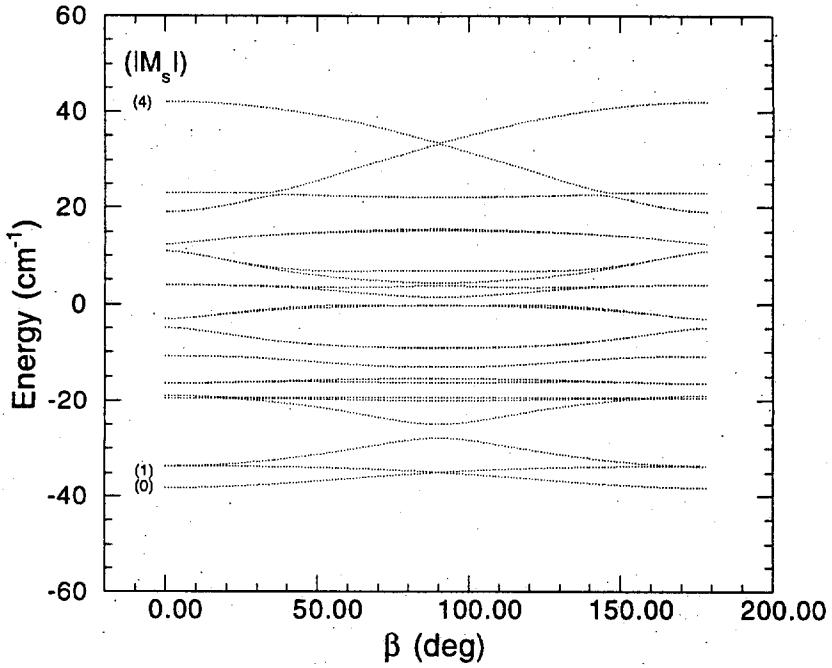

Figure S6. Correlation diagram of the energy levels of the binuclear ferrous ground state including exchange coupling, single-site ZFS and noncollinearity between the two iron atoms. The axial ZFS parameters (D) of the two iron atoms and the exchange coupling (J) are held constant (D_1 = +10 cm^{-1}, D_2 = +5 cm^{-1} and J = -1.5 cm^{-1}). The angle between the two irons varies from 0 to 180 degrees. The spin Hamiltonian used for calculating the levels is given in Eq. 1, with $H_x = H_y = H_z = 0$.

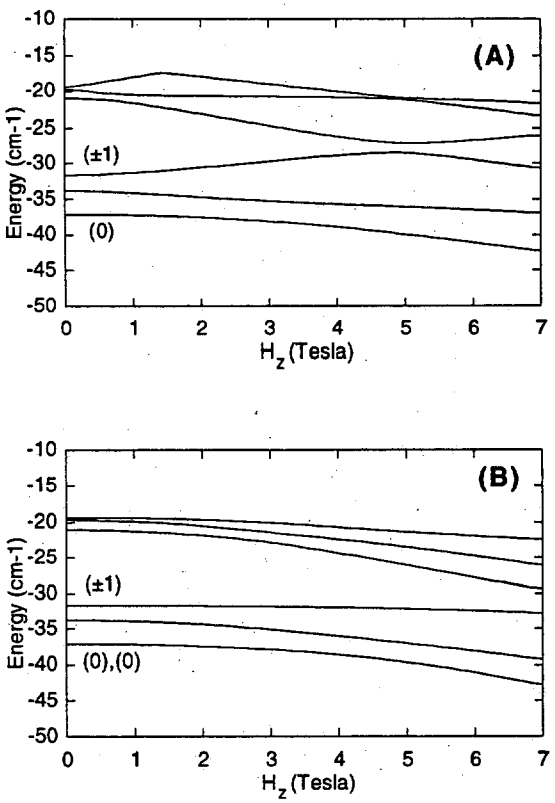

Figure S7. Representative correlation diagrams of the energy splittings of the binuclear ferrous ground and excited sublevels with positive ZFS in the presence of a magnetic field along the z-axis. The axial and rhombic ZFS parameters on the two iron atoms and the exchange coupling are held constant as $D_1 = +10\ cm^{-1}$, $D_2 = +5\ cm^{-1}$, $J = -1.5\ cm^{-1}$. The angle between the two irons (β) is fixed at: (A) $\beta = 45°$ and (B) $\beta = 135°$. The spin Hamiltonian used for calculating the levels is given in Eq. 1, with $H_x = H_y = 0$ and H_z varied from 0 to 7 Tesla.

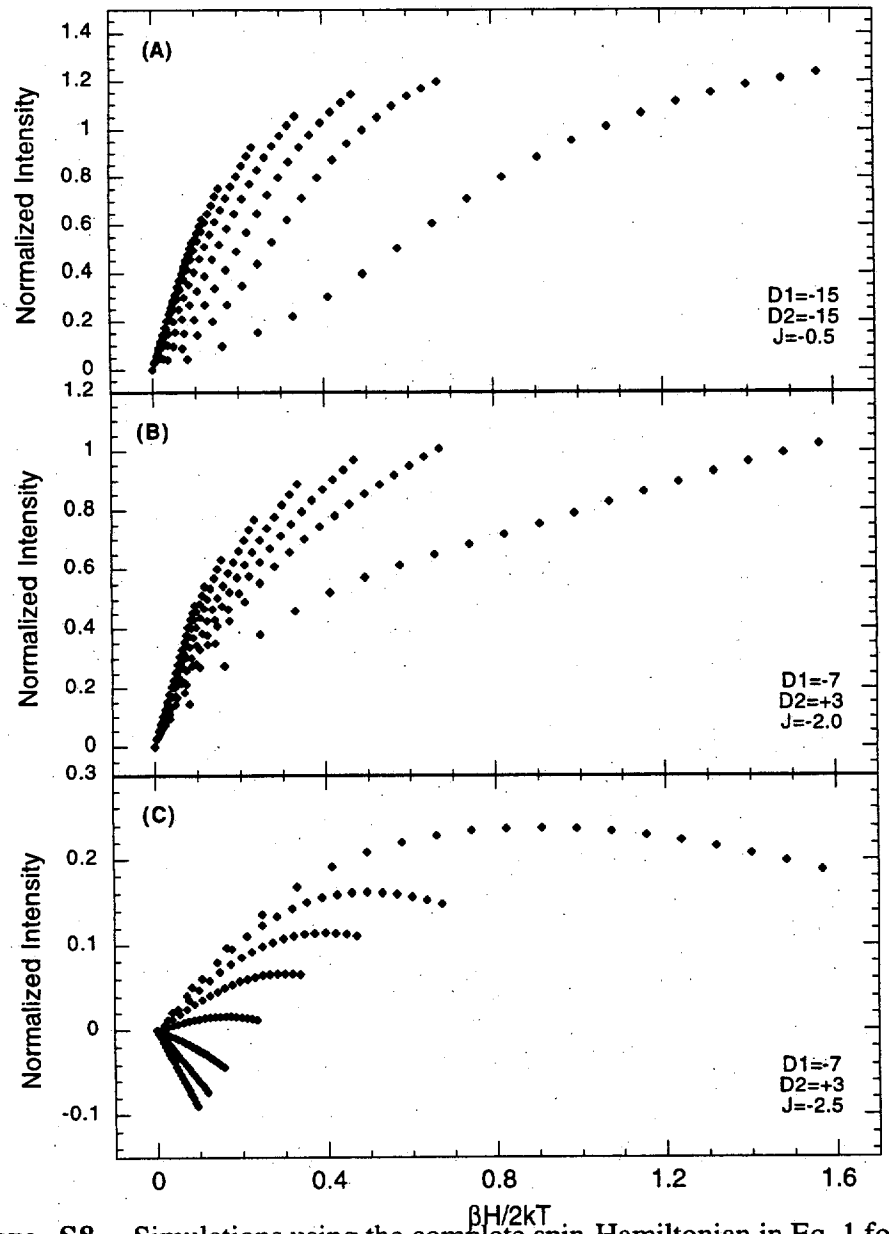

Figure S8. Simulations using the complete spin-Hamiltonian in Eq. 1 for saturation magnetization behavior of the MCD signal in the ligand field region for (A) reduced Δ^9 desaturase at 7,700 cm^{-1}, (B) stearoyl-ACP Δ^9 desaturase at 5,700 cm^{-1}, and (C) stearoyl-ACP Δ^9 desaturase at 9,090 cm^{-1}. The intensity amplitude (symbol) for a range of magnetic fields (0 - 7.0T) at a series of fixed temperatures is plotted as a function of $\beta H/2kT$. Parameters used are listed inset of each figure. Detail of the simulation program is given in Ref 67.